Liquid to Vapor Phase Transition in Excited Nuclei

J. B. Elliott, L. G. Moretto, L. Phair, and G. J. Wozniak
Nuclear Science Division, Lawrence Berkeley National Laboratory, Berkeley, California 94720

L. Beaulieu,[1] H. Breuer,[2] R. G. Korteling,[3] K. Kwiatkowski,[4] T. Lefort,[5] L. Pienkowski,[6] A. Ruangma,[7] V. E. Viola,[5] and S. J. Yennello[7]

(ISiS Collaboration)

[1]*Départment de Physique, Université Laval Québec, Canada G1K 7P4*
[2]*Department of Physics, University of Maryland, College Park, Maryland 20740*
[3]*Department of Chemistry, Simon Fraser University, Burnaby, British Columbia, Canada V5A IS6*
[4]*Physics Division p-23, Los Alamos National Laboratory, Los Alamos, New Mexico 87545*
[5]*Department of Chemistry and IUCF, Indiana University, Bloomington, Indiana 47405*
[6]*Heavy Ion Laboratory, Warsaw University, Warsaw, Poland*
[7]*Department of Chemistry & Cyclotron Laboratory, Texas A&M University, College Station, Texas 77843*
(Received 11 April 2001; revised manuscript received 23 August 2001; published 15 January 2002)

The thermal component of the 8 GeV/c π + Au data of the ISiS Collaboration is shown to follow the scaling predicted by Fisher's model when Coulomb energy is taken into account. Critical exponents τ and σ, the critical point (p_c, ρ_c, T_c), surface energy coefficient c_0, enthalpy of evaporation ΔH, and critical compressibility factor C_c^F are determined. For the first time, the experimental phase diagrams, (p, T) and (T, ρ), describing the liquid vapor coexistence of finite neutral nuclear matter have been constructed.

DOI: 10.1103/PhysRevLett.88.042701 PACS numbers: 25.70.Pq, 05.70.Jk, 24.60.Ky, 64.60.Ak

Nuclear multifragmentation, the breakup of a nuclear system into several intermediate sized pieces, has been frequently discussed in terms of equilibrium statistical mechanics, and of its possible association with a phase transition [1–3]. However, to this point much uncertainty remains regarding its nature, in particular, whether multifragmentation is a phase transition and if so, whether it is associated with the liquid to vapor phase transition. This Letter shows that (i) high quality experimental data contain the signature of a liquid to vapor phase transition through their strict adherence to Fisher's droplet model when modified to account for Coulomb energy; (ii) the two-phase coexistence line is observed via the scaled fragment yields and extends over a large energy/temperature interval up to the critical point; (iii) two critical exponents, as well as the critical temperature, the surface energy coefficient, the enthalpy of evaporation, and the critical compressibility factor can be directly extracted; and (iv) the nuclear phase diagram can be constructed.

In past investigations of the relationship between nuclear multifragmentation and a liquid to vapor phase transition, critical exponents were determined [1,4–7], caloric curves were examined [8], and the observation of negative heat capacities was reported [9]. Other studies showed two general, empirical properties of the fragment multiplicities called reducibility and thermal scaling [3,10,11]. Reducibility, an indication of stochastic fragment production, refers to the observation that for each energy bin the fragment multiplicities are distributed according to a binomial or a Poissonian law. Thus, their multiplicity distributions can be *reduced* to a one-fragment production probability according to a binomial or Poissonian distribution. Thermal scaling refers to the feature that the average fragment yield $\langle N \rangle$ behaves with temperature T as a Boltzmann factor: $\langle N \rangle \propto \exp(-B/T)$.

The features of reducibility and thermal scaling are inherent to any statistical model. In particular, they are present in Fisher's droplet model [12] and will be observed in any system that it describes [7,13]. Fisher's model describes the aggregation of molecules into clusters in a vapor, thus accounting for its nonideality. The abundance of a cluster of size A is given by

$$n_A = q_0 A^{-\tau} \exp\left(\frac{A\Delta\mu}{T} - \frac{c_0 \varepsilon A^\sigma}{T}\right), \tag{1}$$

where $n_A = N_A/A_0$ is the number of droplets N_A of mass A, normalized to the system size A_0; q_0 is a normalization constant depending only on the value of τ [14]; τ is the topological critical exponent; $\Delta\mu = \mu - \mu_l$, and μ and μ_l are the actual and liquid chemical potentials, respectively; $c_0 \varepsilon A^\sigma$ is the surface free energy of a droplet of size A; c_0 is the zero temperature surface energy coefficient; σ is the critical exponent related to the ratio of the dimensionality of the surface to that of the volume; and $\varepsilon = (T_c - T)/T_c$ is the control parameter, a measure of the distance from the critical point, T_c. At coexistence ($\Delta\mu = 0$), Eq. (1) reduces to a Boltzmann factor with a "barrier" $B = c_0 A^\sigma$ (the cost to produce the surface of a cluster of size A) and thermal scaling is observed.

Recently, multifragmentation data from the Indiana Silicon Sphere (ISiS) Collaboration was shown to exhibit both reducibility and thermal scaling [15,16]; thus it follows that Fisher's model may describe the ISiS data. To verify this, the ISiS charge yields from the Alternating Gradient Synchrotron (at BNL) experiment E900a of 8 GeV/c π + Au fragmentation data (see Fig. 1a) were fit to a modified form of Eq. (1) which incorporates, in an approximate manner, the Coulomb energy release when a particle moves from the liquid to the vapor:

$$n_A = q_0 A^{-\tau} \exp\left(\frac{A\Delta\mu + E_{\mathrm{Coul}}}{T} - \frac{c_0 \varepsilon A^{\sigma}}{T}\right), \quad (2)$$

where E_{Coul} is given by

$$E_{\mathrm{Coul}} = \frac{e^2}{4\pi\epsilon_0} \frac{(Z_0 - Z)Z}{r_0[(A_0 - A)^{1/3} + A^{1/3}]} (1 - e^{-x\varepsilon}). \quad (3)$$

Here Z_0 is the charge of the system and $r_0 = 1.2$ fm. This energy vanishes as $x\varepsilon$ at the critical point where no distinction exists between liquid and vapor. The mass of a fragment prior to secondary decay A was estimated by multiplying the measured fragment charge Z by an A/Z ratio of 2 and by a factor of $[1 + (E^*/B_f)]$, where E^* is the reconstructed excitation energy of the event and B_f is the binding energy of the fragment. The temperature T was determined by assuming a degenerate Fermi gas, $T = \sqrt{E^*/a}$ and $a = A_0/\alpha$. To accommodate the empirically observed change in α with excitation energy [17], it is assumed that $\alpha = 8(1 + E^*/B_0)$ [18] with B_0 as the binding energy of the fragmenting system.

Over 500 data points for $1.5 \leq E^* \leq 6.0$ MeV/nucleon and $5 \leq Z \leq 15$ were simultaneously fit to Eq. (2) with the parameters of the modified Fisher model ($\Delta\mu$, x, τ, σ, c_0, and T_c) allowed to vary to minimize chi-squared (see Fig. 1). Fragments with $Z < 5$ were not considered in the fit because (i) Fisher's model expresses the mass/energy of a fragment in terms of bulk and surface energies and this approximation is known to fail for the lightest of nuclei where structure details (shell effects) dominate, and (ii) for the lightest fragments equilibrium and nonequilibrium production cannot always be differentiated. Fragments with $Z > 15$ were not elementally resolved [19], and were also excluded.

While analyses have been performed on other multifragmentation data in the past [20–22], those efforts dealt with inclusive data sets. The present work makes use of the high statistics, exclusive ISiS E900a data set and bins the events

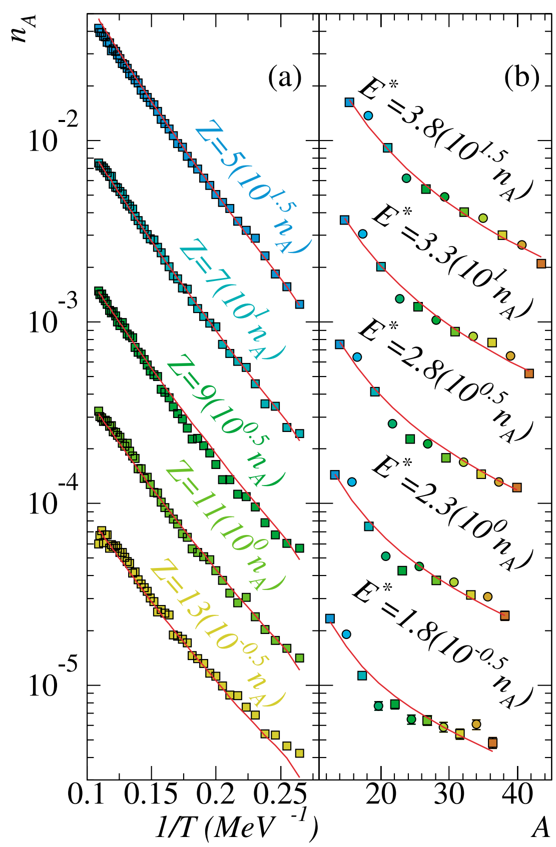

FIG. 1 (color). (a) Arrhenius plots for representative charges, the fragment mass yields versus inverse temperature for the ISIS data. (b) Fragment mass yields for various values of E^*. Solid curves are from a fit to Fisher's model. See Fig. 2 for symbol definition. Error bars are smaller than the size of the points.

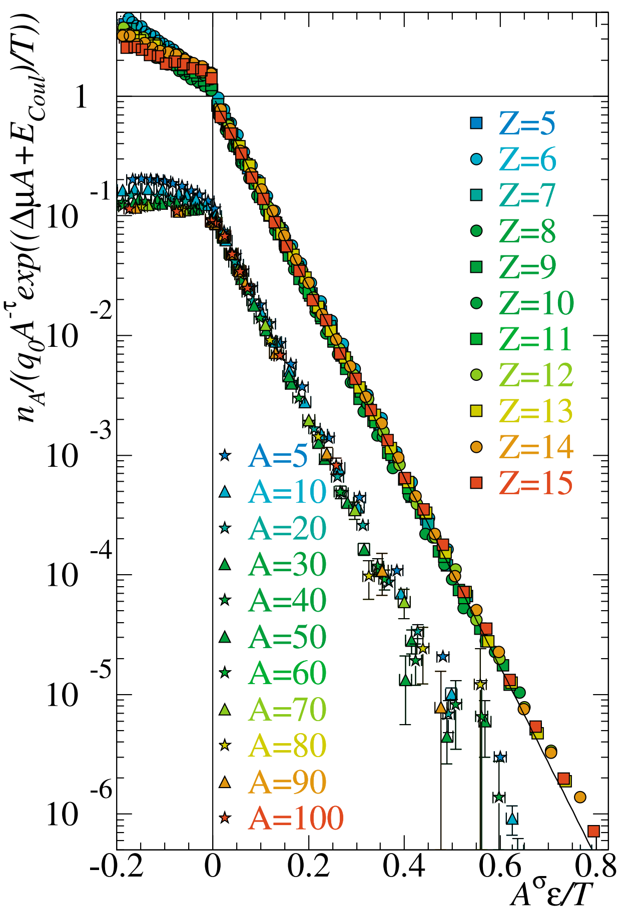

FIG. 2 (color). The scaled yield distribution versus the scaled temperature for the ISiS data (upper) and $d = 3$ Ising model calculation (lower). For the Ising model, the quantity $(n_A/q_0A^{-\tau})/10$ is plotted against the quantity $A^{\sigma}\varepsilon/1.435T$. Data for $T > T_c$ is scaled only as $n_A/q_0A^{-\tau}$.

in terms of their reconstructed excitation energy [23]. In addition, explicit use of Fisher's expressions for the bulk and surface energies and the inclusion of E_{Coul} allows $\Delta\mu$ and c_0 to be determined directly from the data.

The behavior of the data for the (n_A, A, T) surface is reproduced over a wide range in E^* and Z as shown in both Arrhenius plots (Fig. 1a) and fragment yield distributions (Fig. 1b). The results of scaling the data according to Eq. (2) are shown in Fig. 2. The fragment mass yield distribution is scaled by the Fisher's power law prefactor, the bulk term, and the Coulomb energy: $n_A/q_0A^{-\tau} \times \exp[(\Delta\mu A + E_{\mathrm{Coul}})/T]$. This quantity is plotted against the temperature scaled by Fisher's parametrization of the surface energy: $A^\sigma \varepsilon/T$. The scaled data collapse to a single line over 6 orders of magnitude, precisely the behavior predicted by Fisher's model. This line is the liquid-vapor coexistence line, as shown below, and provides direct evidence for the liquid to vapor phase transition in excited nuclei. It may be worth noticing that Fig. 2 represents the first extensive test ever for any physical system of Fisher's formula [Eq. (1)].

To illustrate the generality of this type of scaling, Fig. 2 shows the scaled cluster distributions from a $d = 3$ Ising model calculation [13] a system known to model liquid-vapor coexistence up to T_c. The perfect scaling of the cluster yields according to Eq. (1) demonstrates liquid-vapor-like coexistence up to T_c.

The value of $\tau = 2.18 \pm 0.14$ is in the range predicted by Fisher's model and $\sigma = 0.54 \pm 0.01$ is close to the value expected for a three dimensional system, $\sim 2/3$. The $\Delta\mu = 0.06 \pm 0.03$ MeV/nucleon may indicate that the system is a slightly supersaturated vapor. The value of x is 1.00 ± 0.06. The value of $c_0 = 18.3 \pm 0.5$ MeV is close to the value of the surface energy coefficient of the liquid-drop model: 16.8 MeV. The values of the critical exponents determined here are in agreement with those determined from other multifragmentation data [5,6] and the value of the excitation energy at the critical point $E_c^* = 3.8 \pm 0.3$ MeV/nucleon is in the neighborhood of the value observed in the EOS analysis ($E_c^* \approx 4.75$ MeV/nucleon) [6,7,24]. The two experiments use a different method to distinguish *particles* resulting from the initial projectile-target collision from *fragments* formed afterwards; this difference leads to ${}^{\mathrm{EOS}}E^* \approx 1.2\,{}^{\mathrm{ISiS}}E^*$ [23]. The value of ${}^{\mathrm{EOS}}E_c^*$ corresponds to the steepest decrease in the mass of the largest fragment and to the maximum value of its variance in the EOS data [6,24]. The EOS analysis also relied on the assumptions that $\Delta\mu \approx 0$ and that the effects of the Coulomb energy were small; the present effort tests both assumptions and finds them to be approximately valid. The extracted critical temperature $T_c = 6.7 \pm 0.2$ MeV is comparable to theoretical estimates for small nuclear systems [25,26].

Using the values of the parameters determined above and Eq. (2), the coexistence curve observed in the scaled fragment yields in Fig. 2 can be cast into a more familiar form. Fisher's model assumes that the nonideal vapor can be approximated by an ideal gas of clusters. Accordingly, the quantity n_A is proportional to the partial pressure of a fragment of mass A and the total pressure due to all of the fragments is the sum of their partial pressures: $p/T = \sum n_A$. In the actual experiment, this pressure is virtual; it is the pressure the vapor would have to provide the backflow needed to keep the source at equilibrium. The reduced pressure is given by

$$\frac{p}{p_c} = \frac{T \sum n_A(T)}{T_c \sum n_A(T_c)}. \quad (4)$$

The coexistence line for finite neutral nuclear matter is then obtained by using the $n_A(T, \Delta\mu = 0, E_{\mathrm{Coul}} = 0)$ from Eq. (2) in Eq. (4). This is shown in Fig. 3. Recalling the Clausius-Clapeyron equation $dp/dT = \Delta H/T\Delta V$, one obtains $p/p_c = \exp[\Delta H/T_c(1 - T_c/T)]$ which describes several fluids up to T_c [27]. Fitting the coexistence line and using the above value of T_c gives $\Delta H = 26 \pm 1$ MeV, the enthalpy of evaporation of a cluster from the liquid. This value, after a correction $pV = T$, gives a value for $\Delta E \approx 22$ MeV. Since the gas described by Fisher's model is nonideal, the average cluster is greater in size than a monomer. The average size of a fragment in the region of the p-T coexistence line obtained from Eq. (2) and the experimentally determined parameters is 1.5. Thus the ΔE/nucleon becomes $\approx$15 MeV, remarkably close to the nuclear bulk energy coefficient.

The system's density can be found from $\rho = \sum A n_A$, and the reduced density from

$$\frac{\rho}{\rho_c} = \frac{\sum A n_A(T)}{\sum A n_A(T_c)}. \quad (5)$$

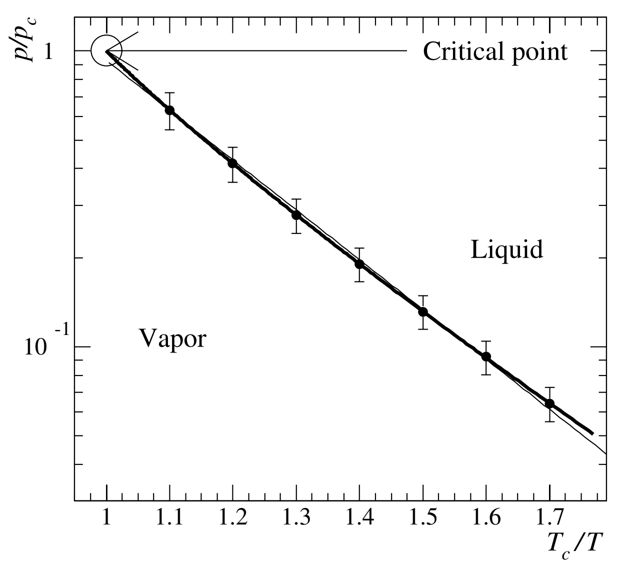

FIG. 3. The reduced pressure-temperature phase diagram: the thick line shows the calculated coexistence line, the points show selected calculated errors, and the thin line shows a fit to the Clausius-Clapeyron equation.

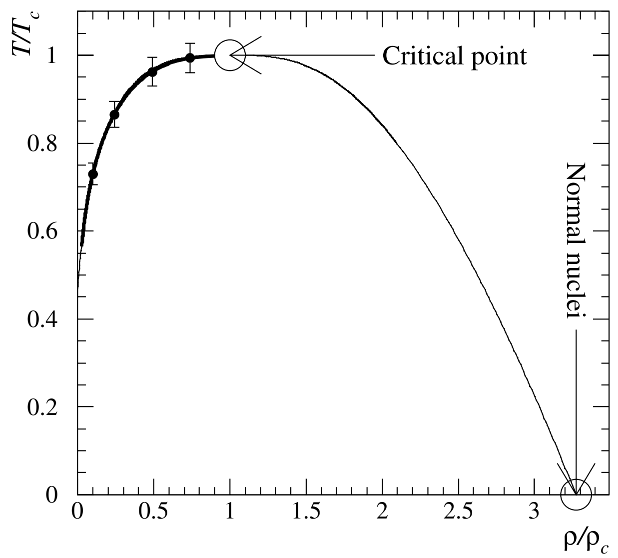

FIG. 4. The reduced density-temperature phase diagram: the thick line is the calculated low density branch of the coexistence curve, the points are selected calculated errors, and the thin lines are a fit to and reflection of Guggenheim's equation.

With $\Delta\mu$ and E_{Coul} set to 0 in Eq. (2), Eq. (5) yields the low density branch of the coexistence curve of finite neutral nuclear matter, shown in Fig. 4. Following Guggenheim it is possible to determine the high density branch as well: empirically, the ρ/ρ_c-T/T_c coexistence curves of several fluids can be fit with the function [28]

$$\frac{\rho_{l,v}}{\rho_c} = 1 + b_1\left(1 - \frac{T}{T_c}\right) \pm b_2\left(1 - \frac{T}{T_c}\right)^{1/3}, \quad (6)$$

where the parameter b_2 is positive (negative) for the liquid ρ_l (vapor ρ_v) branch. It was later recognized that the power of 1/3 was the critical exponent β. Using Fisher's model, β can be determined from τ and σ: $\beta = (\tau - 2)/\sigma$ [12]. For this work $\beta = 0.33 \pm 0.25$. Using this value of β and fitting the coexistence curve from the ISiS E900a data with Eq. (6) one obtains an estimate of the full ρ_v branch of the coexistence curve and changing the sign of b_2 gives the full ρ_l branch of the coexistence curve of finite neutral nuclear matter. If normal nuclei exist at the $T = 0$ point of the coexistence curve and the parametrization of the coexistence curve in Eq. (6) is used, then the critical density is found to be $\rho_c \sim 0.3\rho_0$. The critical compressibility factor $C_c^F = p_c/T_c\rho_c$ is 0.25 ± 0.06, in agreement with the values for several fluids [29]. Using T_c and ρ_c from above in combination with C_c^F gives a critical pressure of $p_c \sim 0.07$ MeV/fm^3.

In conclusion, the ISiS data contain the signature of a liquid to vapor phase transition via their strict adherence to Fisher's model.Through Fisher's scaling of the fragment yield distribution (Fig. 2), the two-phase coexistence line has been determined over a large energy/temperature interval extending up to the critical point. Fisher's formula [Eq. (1)] has been extensively tested and verified for the first time for any physical system. The critical exponents τ and σ as well as the critical temperature T_c, the surface energy coefficient c_0, the enthalpy of evaporation ΔH, and the critical compressibility factor C_c^F have been extracted and found to agree with accepted values. Finally, p_c and ρ_c have also been determined, giving the first complete experimental determination of the critical point and the full phase diagram of finite neutral nuclear matter.

We thank C. M. Mader for her input and Ising calculations. This work was supported by the U.S. Department of Energy, the National Science Foundation, the National Science and Engineering Research Council of Canada, the Polish State Committee for Scientific Research, Indiana University Office of Research, the University Graduate School, Simon Fraser University, and the Robert A. Welch Foundation.

[1] J. E. Finn *et al.,* Phys. Rev. Lett. **49**, 1321 (1982).
[2] P. J. Siemens, Nature (London) **305**, 410 (1983).
[3] L. G. Moretto *et al.,* Phys. Rep. **287**, 249 (1997).
[4] M. L. Gilkes *et al.,* Phys. Rev. Lett. **73**, 1590 (1994).
[5] M. D'Agostino *et al.,* Nucl. Phys. **A650**, 328 (1999).
[6] J. B. Elliott *et al.,* Phys. Rev. C **62**, 064603 (2000).
[7] J. B. Elliott *et al.,* Phys. Rev. Lett. **85**, 1194 (2000).
[8] J. Pochodzalla *et al.,* Phys. Rev. Lett. **75**, 1040 (1995).
[9] M. D'Agostino *et al.,* Phys. Lett. B **473**, 219 (2000).
[10] L. Beaulieu *et al.,* Phys. Rev. Lett. **81**, 770 (1998).
[11] L. G. Moretto *et al.,* Phys. Rev. C **60**, 031601 (1999).
[12] M. E. Fisher, Physics (N.Y.) **3**, 255 (1967).
[13] C. M. Mader *et al.,* nucl-th/0103030.
[14] H. Nakanishi *et al.,* Phys. Rev. B **22**, 2466 (1980).
[15] L. Beaulieu *et al.,* Phys. Rev. Lett. **84**, 5971 (2000).
[16] L. Beaulieu *et al.,* Phys. Rev. C **63**, 031302 (2001).
[17] K. Hagel *et al.,* Nucl. Phys. **A486**, 429 (1988).
[18] A. H. Raduta *et al.,* Phys. Rev. C **55**, 1344 (1997).
[19] K. Kwiatkowski *et al.,* Nucl. Instrum. Methods Phys. Res., Sect. A **360**, 571 (1995).
[20] A. S. Hirsch *et al.,* Phys. Rev. C **29**, 508 (1984).
[21] A. L. Goodman *et al.,* Phys. Rev. C **30**, 851 (1984).
[22] M. Mahi *et al.,* Phys. Rev. Lett. **60**, 1936 (1988).
[23] T. Lefort *et al.,* Phys. Rev. Lett. **83**, 4033 (1999).
[24] J. A. Hauger *et al.,* Phys. Rev. C **57**, 764 (1998).
[25] H. R. Jaqaman *et al.,* Phys. Rev. C **29**, 2067 (1984).
[26] P. Bonche *et al.,* Nucl. Phys. **A436**, 265 (1985).
[27] E. A. Guggenheim, *Thermodynamics* (North-Holland, Amsterdam, 1993), 4th ed.
[28] E. A. Guggenheim, J. Chem. Phys. **13**, 253 (1945).
[29] C. S. Kiang, Phys. Rev. Lett. **24**, 47 (1970).